Carbohydrate Polymers 110 (2014) 135–141

Contents lists available at ScienceDirect

Carbohydrate Polymers

journal homepage: www.elsevier.com/locate/carbpol

Construction of serum resistant micelles based on heparosan for targeted cancer therapy

Jing-Xiao Chen[a,b], Miao Zhang[a], Wen Liu[a], Guo-Zhong Lu[c,**], Jing-Hua Chen[a,b,*]

[a] School of Pharmaceutical Science, Jiangnan University, Wuxi 214122, PR China
[b] Key Laboratory of Carbohydrate Chemistry and Biotechnology, Ministry of Education, Jiangnan University, Wuxi 214122, PR China
[c] Department of Burns & Plastic Surgery, Wuxi Third Renmin Hospital, Wuxi 214041, PR China

ARTICLE INFO

Article history:
Received 22 January 2014
Received in revised form 25 March 2014
Accepted 26 March 2014
Available online 5 April 2014

Keywords:
Heparosan
Serum resistance
Micelle
Drug delivery

ABSTRACT

A novel micelle based on heparosan and deoxycholic acid (DOCA) conjugate (HD) as drug carrier was reported here. As the surface was negatively charged, this micelle could resist serum adsorption, showing favorable stability. Moreover, fluorescence observation confirmed that it was able to deliver model hydrophobic drug doxorubicin (DOX) into HeLa cells efficiently. The DOX-loaded micelles showed sustained release behavior at pH 7.4, and accelerated release behavior at pH 5.0 or in the presence of β-glucuronidase, which over-expressed in tumor cells. *In vitro* cytotoxicity assay demonstrated that the half-maximal inhibitory concentration (IC50) of DOX-loaded micelles against HeLa cells was much lower than that of COS7 cells, showing significant therapeutic distinction between tumor cells and normal cells. Combining with the good biocompatibility and biodegradability of heparosan, this micelle may be promising in clinical application for targeted drug delivery.

1. Introduction

Drug carriers aim to improve the efficacy and reduce systemic side effects of drugs especially in the field of cancer chemotherapy (Duncan, 2003; Ferrari, 2005; Kataoka, Harada, & Nagasaki, 2001). Although numerous potent drugs have been developed, their clinical application still faces with intractable problems, such as poor water solubility, lack of specificity, short blood circulation time and limited bioavailability (Brigger, Dubernet, & Couvreur, 2002; Peer et al., 2007). To overcome these obstacles, a promising strategy is to use self-assembly micelle as a carrier to achieve on-target delivery of drugs (Langer & Tirrell, 2004; Torchilin, 2001). As is known, the size, shape, surface charge and surface functional groups strongly influence the circulation of nanoparticles in bloodstream (Stark, 2011; Wang, He, Zhang, Zhao, & Feng, 2013). Nevertheless, micelle has exhibited many distinctive advantages in the regulation of these factors (Rosler, Vandermeulen, & Klok, 2001). Morphological features of micelle, like size and shape can be regulated by adjusting the structure and hydrophilic/hydrophobic balance of the polymeric amphiphiles, and micelle can be easily endowed with specific surface properties by binding functional groups (Blanazs, Armes, & Ryan, 2009; Riess, 2003; Xu, Chen, Cheng, Zhang, & Zhuo, 2012). Poly (ethylene glycol) (PEG) has been commonly introduced to prolong the circulation time and improve the stability and bioavailability of micelles, because of its capability of resisting protein adsorption (Koo et al., 2011; Moghimi, Hunter, & Murray, 2001; Otsuka, Nagasaki, & Kataoka, 2003). However, the utilization of PEG is yet limited by its artificial nature, including non-biodegradability, exogenous nature and latent long-term renal toxicity (Caliceti & Veronese, 2003; Karmali & Simberg, 2011; Simpson, Agrawal, Balinski, Harkness, & Cliffel, 2011). These facts therefore urge the development of novel materials for substituting PEG.

Polysaccharides are highly abundant natural polymers from different origins (*e.g.* plant origin, microbial origin and animal origin) (Janes, Calvo, & Alonso, 2001). Since polysaccharides possess many inherent properties such as biocompatibility, biodegradability, low toxicity and ease of chemical modification, they have been well reported for drug delivery (Baldwin & Kiick, 2010; Liu, Jiao, Wang, Zhou, & Zhang, 2008; Mizrahy & Peer, 2012). Recently, heparosan, a heparin precursor isolated from *Escherichia. coli* K5, has attracted much research attention (Raman, Mencio, Desai, & Kuberan, 2013; DeAngelis, 2013). It can not only be used for *in vitro* chemoenzymatic synthesis of heparin, but also be regarded as "self" by host-defense system *in vivo*, and thus

* Corresponding author at: School of Pharmaceutical Science, Jiangnan University, Wuxi 214122, PR China. Tel.: +86 510 85911900; fax: +86 510 85329042.
** Corresponding author. Tel.: +86 510 82603338; fax: +86 510 82603338.
E-mail addresses: luguozhong@hotmail.com (G.-Z. Lu), jhchenwhut@126.com (J.-H. Chen).

http://dx.doi.org/10.1016/j.carbpol.2014.03.084
0144-8617/

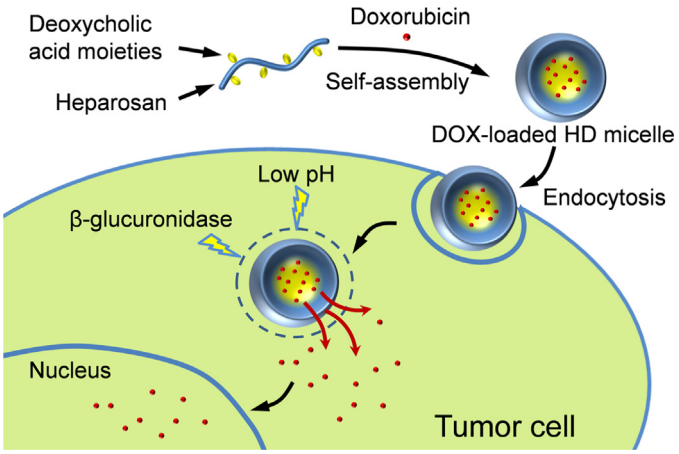

Scheme 1. Schematic illustration of the formation of self-assembled HD micelles and intracellular drug delivery.

be expected as non-immunogenic (Blundell, Roberts, Sheehan, & Almond, 2009; Chen et al., 2005; Li et al., 2013). This fact is employed by certain pathogenic bacteria to escape from immune clearance (Clarke, Esumeh, & Roberts, 2000; Volpi, 2004; Wang, Zhang, McCallum, & Linhardt, 2010). More interestingly, a recent report has demonstrated that heparosan has greater cellular uptake efficiency than heparin, because of its non-sulfation nature (Raman et al., 2013). This feature of heparosan eliminates heparin's inherent drawbacks such as bleeding complications and thrombocytopenia, suggesting favorable biosecurity. Moreover, this property also eliminates the broad protein binding capability of heparin, avoids the opsonization in the blood stream and leads to prolonged circulation half-life of heparosan. Besides, heparosan can be degraded by β-glucuronidase over-expressed in tumor cells (Barzu, van Rijn, Petitou, Tobelem, & Caen, 1987; DeAngelis, 2013; Grinda, Clarhaut, Renoux, Tranoy-Opalinski, & Papot, 2012). By these inspiring results, heparosan and its derivatives may serve as potential substitutes of PEG for drug delivery.

Herein, we reported a self-assembly micelle based on heparosan and deoxycholic acid (DOCA) conjugate (HD) as a novel drug carrier. The amphiphilic HD was obtained by covalently linking DOCA as the hydrophobic moiety to the main chain of heparosan. Therefore, the HD could self-assemble into core-shell micelles in aqueous medium with DOCA aggregated in the core and negatively charged heparosan gathered on the shell (Scheme 1). It is expected that the micelle can encapsulate model drug doxorubicin (DOX) in the hydrophobic core, provide protection to the drug in physiological milieu containing serum, and then deliver drug into tumor cells. The *in vitro* drug release behavior, cytotoxicity as well as cellular uptake ability were investigated.

2. Experimental

2.1. Materials

The strain of *E. coli* K5 engineering bacteria was frozen and stored in the Lab. Deoxycholic acid (DOCA), n-hexane, ethylenediamine (EDA), tris base and ethanol were purchased from Shanghai Reagent Chemical Co. (China) and used directly. *N,N′*-dicyclohexylcarbodiimide (DCC), *N,N′*-diisopropylcarbodiimide (DIC) and *N*-hydroxysuccinimide (NHS) were provided by Aladdin Regent Co. (China) and used as received. Tetrahydrofuran (THF), dimethylformamide (DMF), formamide and triethylamine (TEA) were purchased from Shanghai Reagent Chemical Co. (China) and distilled prior to use. Doxorubicin hydrochloride (DOX·HCl) was obtained from Zhejiang Hisun Pharmaceutical Co. (China) and used as received. β-glucuronidase (1000 U/mg) was purchased from Sigma–Aldrich Co., and used directly. Dulbecco's modified eagle medium (DMEM), RPMI-1640 medium, fetal bovine serum (FBS), 3-[4,5-dimethylthiazol-2-yl]-2,5-diphenyltetrazoliumbromide (MTT), trypsin, 4′,6-diamidino-2-phenylindole (DAPI) and penicillinestreptomycin were purchased from Invitrogen Corp. DEAE-Sepharose gel was purchased from GE Healthcare Bioscience Bioprocess Corp. All other reagents and solvents were of analytical grade and used directly.

2.2. Synthesis of N-deoxycholylethylenediamine (DOCA-NH_2)

N-deoxycholylethylenediamine (DOCA-NH_2) was synthesized according to a reported method (Park et al., 2004). Briefly, DOCA (5.9 g, 15 mmol), DCC (4.1 g, 20 mmol) and NHS (2.3 g, 20 mmol) were dissolved in dry THF (50 mL). The mixture was reacted overnight under nitrogen atmosphere at room temperature. After removing insoluble dicyclohexylurea, the filtrate was poured into n-hexane to obtain the precipitated succinimido DOCA. Then, succinimido DOCA (4 g, 10 mmol) was dissolved in DMF (10 mL) and the solution was added dropwise into ethylenediamine (60 mL). After the reaction under nitrogen atmosphere for 6 h, the solution was concentrated and then poured into distilled water to obtain the precipitate. The product was washed with distilled water and dried under vacuum. The chemical structure and ^{1}H NMR spectrum of DOCA-NH_2 was shown in Fig. S1 (Supplementary data).

2.3. Synthesis of HD

The preparation of heparosan was performed according to our previous report (Zhang et al., 2012). Briefly, *E. coli* K5 was amplified by a high cell density fermentation method and heparosan was isolated and purified by ethanol precipitation followed by ion-exchange chromatography (see purification and characterization details in the supplementary data).

Thereafter, heparosan (100 mg), DIC (0.47 mL, 3 mmol) and NHS (0.345 g, 3 mmol) were dissolved in formamide (5 mL) with gentle heating and stirring. After activating the carboxyl acid groups for 30 min, 5 mL of DMF solution containing DOCA-NH_2 (1 g, 2.3 mmol) was added. After the reaction for 36 h, the solution was concentrated by rotary evaporation and cold acetone was then added to precipitate the crude product, precipitates were washed carefully by acetone to remove excess DOCA-NH_2. The product was dissolved in distilled water and put into a dialysis tube (MWCO 3500 Da) and subject to dialysis against distilled water to remove impurities. The expected amphiphilic HD was collected by lyophilization. The synthesis route of HD was shown in Fig. 1. The ^{1}H NMR spectra of heparosan and HD were respectively shown in Fig. S2 (Supplementary data).

2.4. Determination of critical micelle concentration (CMC)

The CMC value of HD was estimated by fluorescence spectra, which record on a RF-5301PC fluorescence spectrophotometer (Shimadzu, Japan) by using pyrene as the hydrophobic fluorescent probe. Aliquots of pyrene solutions (6×10^{-5} M in acetone, 30 μL) were added to containers, and the acetone was allowed to evaporate. Subsequently, a series of HD solution (3 mL) of different concentrations ranging from 0.01 mg/L to 1000 mg/L were added to containers and sonicated (100 W) for 15 min. The solutions were then kept in a thermostatic water bath (37 °C) overnight in the dark to reach the solubilization equilibrium of pyrene. Emission was carried out at 390 nm, and excitation spectra were recorded ranging from 280 to 380 nm. The slit width of both excitation and emission was 3 nm. From the pyrene excitation spectra, the fluorescence intensity ratio of the third and first vibronic bands (I_3/I_1)

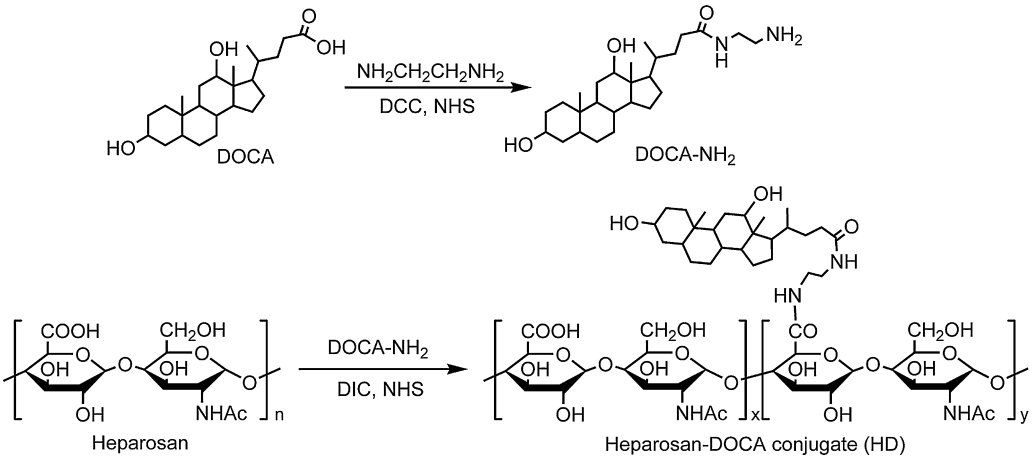

Fig. 1. Synthetic route for heparosan–DOCA conjugate (HD).

was plotted against the logarithm of the HD concentrations. The CMC value was determined from the intersection of the tangent to the curve at the inflection with the horizontal tangent through the points at low concentration. See Fig. S3 in the supplementary data.

2.5. Micelle formation, size distribution and morphological observation

The micelles of HD were prepared by dissolving HD in distilled water (pH 7.0) directly, and the concentration was higher than the CMC value measured above. The average size, size distribution and ζ-potential of self-assembled micelles and DOX-loaded micelles in aqueous solution were determined by dynamic light scattering (DLS) techniques with a Zetasizer Nano ZS apparatus (Malvern Instruments, UK) at 37 °C. The concentration of the sample was 1 mg/mL. The morphology of micelles and DOX-loaded micelles was observed by transmission electron microscopy (TEM) on a JEM-2100 (JEOL, Japan) instrument with an acceleration voltage of 80 kV. The sample was prepared by dripping a drop of sample solution (1 mg/mL) on a copper grid. After the deposition, excess solution was blotted away, the sample was stained with phosphotungstic acid aqueous solution (0.2%, w/v), and then dried in air. To investigate the serum resistance and stability of micelles, 10% FBS (v/v) was added into sample solutions and then incubated at 37 °C for 1 h before it was used for the measurements.

2.6. Drug loading and in vitro drug release

The DOX-loaded micelles were prepared by dialysis method. Briefly, DOX·HCl (5 mg) and TEA (1 mL) were dissolved in 4 mL of formamide/DMF (3/1, v/v) with stirring in the dark overnight, followed by the addition of HD (20 mg). The solution was put into a dialysis tube (MWCO 3500 Da) and subjected to dialysis against PBS (pH 7.4) for 24 h, the PBS was replaced every 4 h to remove organic solvents and unloaded drug. After drug loading, the solution was divided into 4 parts, three of which were respectively put into dialysis tubes for drug release study, and the remaining one was lyophilized. Two tubes containing DOX-loaded micelles were respectively immersed into 10 mL of PBS of pH 7.4 and pH 5.0 at 37 °C to evaluate the influence of pH value. To evaluate the enzymatic drug release behavior, 1 mg of β-glucuronidase was added into the last dialysis tube containing DOX-loaded micelles. After the enzymatic hydrolysis of heparosan for 30 min at 37 °C, the tube was subjected to dialysis in PBS (pH 7.4). At the setting interval, the sample solution was withdrawn and fresh PBS of relevant pH was replenished after each sampling. The amount of released drug was measured by UV–vis spectrophotometer (UV-2550, Shimadzu, Japan) at 497 nm. Each value was averaged from three independent experiments. The mass of drugs loaded in micelles include the total cumulative mass of released drug and the unreleased drug, which remains in the micelles. To determine the loading amount of DOX in the micelles, the lyophilized DOX-loaded micelle sample of a known amount was dissolved in 1 mL of formamide/DMF solution (1/1, v/v). The UV absorbance was obtained at 480 nm. The encapsulation efficiency (EE) and drug loading level (DL) of the DOX-loaded micelles were calculated as follows:

$$\mathrm{EE}(\%) = \frac{\text{mass of loaded drug}}{\text{mass of feed drug}} \times 100$$

$$\mathrm{DL}(\%) = \frac{\text{mass of loaded drug}}{\text{mass of drug loaded micelle}} \times 100$$

2.7. Cell culture

Human cervix carcinoma (HeLa) cells were incubated in RPMI-1640 medium containing 10% FBS and 0.1% antibiotics (penicillin-streptomycin, 10,000 U/mL). Transformed African green monkey SV40-transformed kidney fibroblast (COS7) cells were incubated in DMEM medium with 10% FBS and 0.1% antibiotics (penicillin-streptomycin, 10,000 U/mL) at 37 °C in a humidified atmosphere containing 5% CO_2.

2.8. In vitro cytotoxicity assay

The cytotoxicity assay was performed against HeLa and COS7 cells by MTT assay. Briefly, HeLa and COS7 cells were respectively seeded in 96-well plates at a density of 8000 cells/well and incubated in 100 μL of complete medium for 12 h prior to adding HD. After the incubation for 2 days, the medium in each well was replaced by 100 μL of MTT solution (0.5 mg/mL in PBS), and further incubated for 4 h. After that, the medium was removed and DMSO (100 μL) was added to each well. The optical density values were measured at 570 nm by using a Multiskan MK3 microplate reader (Thermo, USA). The relative cell viability was calculated as follow:

$$\text{Cell viability}(\%) = \frac{\mathrm{OD}_{\mathrm{sample}}}{\mathrm{OD}_{\mathrm{control}}} \times 100$$

where $\mathrm{OD}_{\mathrm{control}}$ is obtained in the absence of HD and $\mathrm{OD}_{\mathrm{sample}}$ is obtained in the presence of HD.

The cytotoxicity of DOX-loaded micelles was measured by the same method, and DOX solution with containing 5% (v/v) DMSO as the co-solvent was used as the positive control.

2.9. Cellular internalization of DOX-loaded micelles

HeLa and COS7 cells were respectively seeded in 24-well plates and incubated in 1 mL of complete medium for 12 h. After that, DOX-loaded micelles dispersed in culture medium (10 mg/L, equivalent to 1.67 mg/L free DOX) containing 10% FBS were added and the cells were incubated for another 1 h. The medium was then removed and gently washed with PBS for several times. Cells were fixed for 15 min in 4% paraformaldehyde water solution at room temperature and then stained by blue fluorescent dye DAPI (0.2 μg/mL in water stock solution) for 10 min. After removing the medium and washing 3 times with PBS, the cells were viewed under a DMIL LED inverted fluorescence microscope (Leica, Germany).

3. Results and discussion

3.1. Synthesis and characterization of HD

For the synthesis of HD, DOCA was initially connected with ethylenediamine to introduce a primary amine group, and then chemically coupled with heparosan. The synthesis route of HD was shown in Fig. 1. Since heparosan could be produced in large quantities by fermentation method, it suggested that HD has a steady and reliable source. The chemical structures of heparosan and HD were respectively identified by ^{1}H NMR (Fig. S2). As shown in Fig. S2a, the characteristic proton peaks of heparosan was consistent with the result reported previously (Zhang et al., 2012). After the conjugation, ^{1}H NMR was operated in two different solvent systems including D2O and CD_3OD/D_2O (v/v, 1:1) to identify the structure of HD. Wherein, CD_3OD/D_2O is an available solvent for dissolving both hydrophilic heparosan chain and hydrophobic DOCA moieties. As shown in Fig. S2c, characteristic proton peaks of both heparosan and DOCA are visible when use CD_3OD/D_2O as the solvent, implying that HD was successfully synthesized. As comparison, the characteristic proton peaks of DOCA (0.62–2.3 ppm) are absent, but the peaks of heparosan are existing in the spectrum operated in D_2O (Fig. S2b). Since DOCA hardly dissolved in water, this result implied the micellization of HD with hydrophobic DOCA moieties enwrapped into the core and hydrophilic heparosan covered on the shell. The characteristic proton peaks of DOCA (0.62 ppm, 21-CH_3) and heparosan (5.31 ppm, 1-H, GlcNAc) used for calculating the degree of substitution (DS) were labeled, as shown in Fig. S2 (See details in supplementary data). The DS of DOCA to heparosan calculated from the peak integration ratio was 0.29 per a disaccharide repeating unit.

3.2. Preparation and characterization of micelles

The HD could self-assemble into micelles in aqueous medium at a fixed concentration, which was verified by the fluorescence technique using pyrene as the hydrophobic probe. As shown in Fig. S3a, the fluorescence intensity of pyrene in the excitation spectra increases with the elevation of HD concentration. Simultaneously, a shift of peak location from 335 nm (I_1) to 339 nm (I_3) was observed clearly from the spectra. This changed photo-physical property attributes to the preferential partition of pyrene from the hydrophilic outer medium into the hydrophobic inner core, indicating the micellization of HD in aqueous solution. The defined critical micelle concentration (CMC) value of HD was determined from the tangent to the curve at the inflection intersected with the horizontal tangent at low concentration (Fig. S3b), and the CMC value is 19.5 mg/L. This low CMC value indicated the designed micelle of HD was stable and could be utilized in a diluted milieu, such as bloodstream.

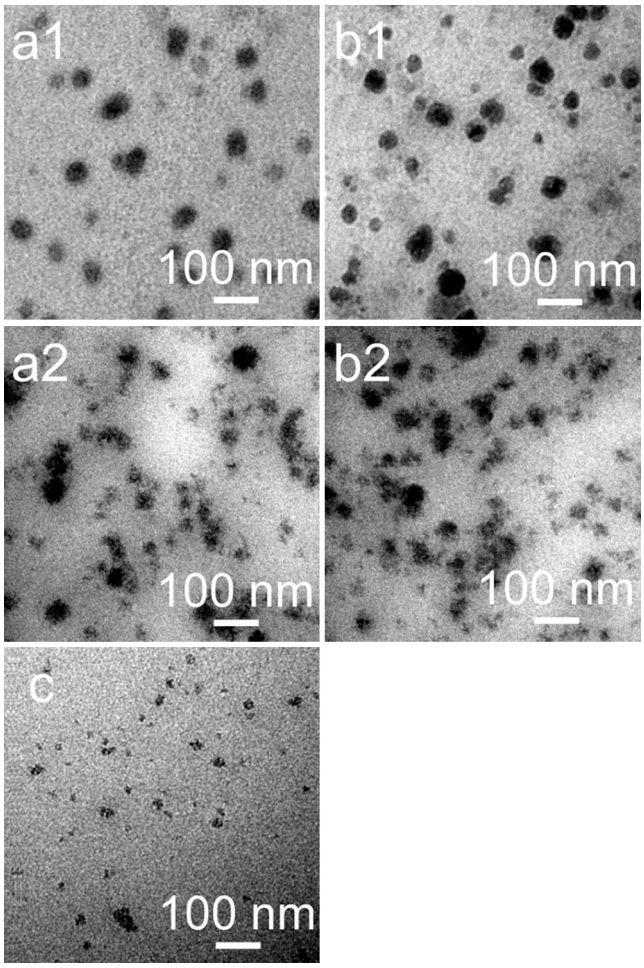

Fig. 2. TEM images of (a) HD micelles, (b) DOX-loaded micelles in PBS solution (1 mg/mL) and (c) 10% FBS; (a1, b1) in the absence of 10% FBS and (a2, b2) in the presence of 10% FBS.

The morphologies of the self-assembly micelles and DOX-loaded micelles were observed by TEM respectively, as shown in Fig. 2. It was found in Fig. 2a1 that the designed amphiphilic HD is able to aggregate in aqueous solution and form well-dispersed micelles with spherical shape. Its size was estimated to be about 50 nm from the TEM image. Fig. 2b1 showed the TEM image of DOX loaded micelles. Clearly, micelles remain spherical shape and dispersibility after loading DOX into the hydrophobic core, but the size is slightly larger (~70 nm) as well as the contrast is higher than that of HD micelles without loading DOX. This indicated the core region of the micelle was more compact, and further illustrated the hydrophobic drug was encapsulated in core of micelles. To evaluate the stability of micelles, fetal bovine serum (FBS) was added into the solution of micelles. As shown in Fig. 2a2 and b2, both HD micelles and DOX-loaded micelles keep their shape in the solution containing 10% FBS. Except micelles, floccules of FBS aggregation was observed as compared with the TEM image of 10% FBS (Fig. 2c). Noted that the agglomeration of micelles was not found in the visual field of either HD micelles or DOX-loaded micelles. These phenomena showed that HD micelles had good serum resistant capability and may offer drug improved circulation period.

Additionally, dynamic light scattering (DLS) measurements further illustrated the stability of HD micelle, as shown in Fig. 3. After the addition of FBS, the size distribution results of either HD micelles (Fig. 3a1 and a2) or DOX-loaded micelles (Fig. 3b1

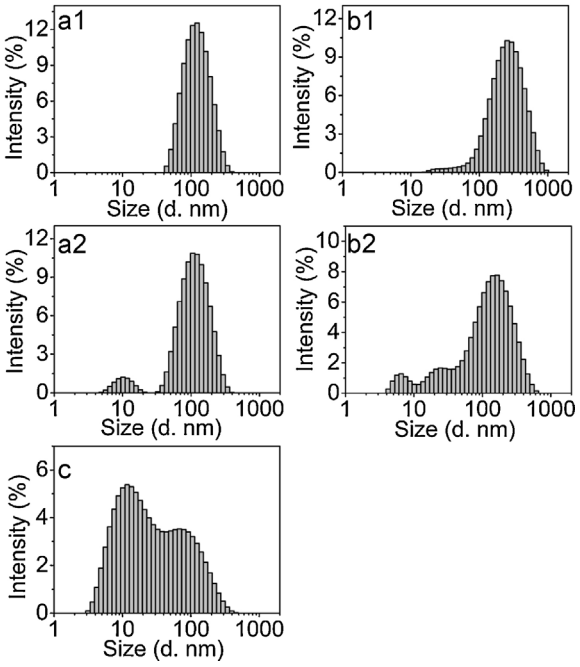

Fig. 3. Size distributions of (a) HD micelles, (b) DOX-loaded micelles and (c) 10% FBS detected by DLS; (a1, b1) in the absence of 10% FBS and (a2, b2) in the presence of 10% FBS.

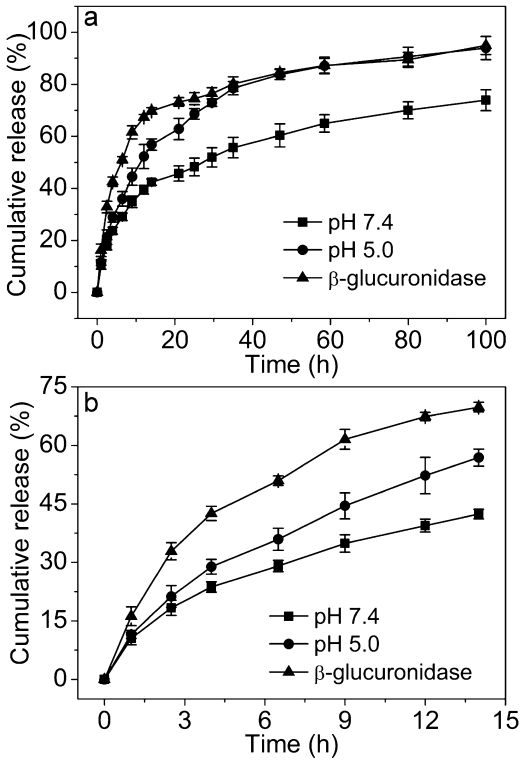

Fig. 4. Drug release profiles of DOX-loaded micelles at pH 7.4, pH 5.0 and in the presence of β-glucuronidase for (a) a week and (b) the initial 14 h. Error bars represent standard deviation of 3 independent replicates for the test.

and b2) showed no-significant variation. As compared with the size distribution result of 10% FBS (Fig. 3c), the peak found around 10 nm in DLS histograms of micelles was due to the aggregation of FBS. This phenomenon was consistent with TEM observation, illustrating that the serum was hard to be adsorbed onto the surface of HD micelles and DOX-loaded micelles. Likewise, the size of DOX-loaded micelles is larger than that of HD micelles. The mean size of HD micelles and DOX-loaded micelles were measured to be 110.8 nm (PDI = 0.207) and 211.4 nm (PDI = 0.254) respectively (Table S1, supplementary data). This result allowed the micelle to share nano-dimensional feature and accumulate in tumor tissue by the EPR effect. The difference of size between TEM observation and DLS detection is due to these micelles will shrink in dried state, showing that HD micelle possesses favorable capability to store water in the shell region. The ζ-potential of HD micelles and DOX-loaded micelles were measured to be −28.1 mV and −31.4 mV respectively (Table S1). This was due to heparosan gathered on the shell region of micelles, leading to the micelles show negatively charged property. Thus, the HD micelles possess favorable stability in serum solution, suitable size and surface charge, showing a potential application as the substitute of PEG for drug delivery.

3.3. DOX-loaded micelles and in vitro drug release

The drug loading capability is the precondition of applying micelle as the drug carrier. Herein, hydrophobic DOX was chosen as the model drug to evaluate the drug encapsulation efficiency (EE) and drug loading level (DL) of micelles. The encapsulation of DOX was simultaneously achieved along with the formation of micelles by dialysis method. The EE and DL values of DOX-loaded micelles in this study were measured to be 62.66% and 16.71% respectively (Table S1). The encapsulation of DOX into the HD micelles was probably attributed to the combined effect of hydrophobic interaction and electrostatic attraction, which divided the loading DOX into two parts of the micelles. On the one hand, DOX was loaded into the core region of micelles because of the hydrophobic interaction. On the other hand, the shell of HD micelles gathering many carboxyl groups of heparosan, which resulting in the micelle bears negative charge, and adsorbing another part of DOX in the shell region of micelles through the electrostatic attraction between carboxyl groups and amino group in the molecule of DOX.

The drug release behavior of DOX-loaded micelles was investigated *in vitro*. The PBS of pH 7.4 was used to imitate the blood and PBS of pH 5.0 to imitate the milieu of tumor site. Besides, in another group, β-glucuronidase was added for simulating lysosomes of tumor cells. As shown in Fig. 4, release profiles showed sustained release behaviors of DOX at pH 7.4 and pH 5.0. The accumulated release rate of DOX at pH 7.4 and pH 5.0 were 36.4% and 46.9% in the initial 10 h (Fig. 4b), and reach 73.9% and 93.9% after 100 h (Fig. 4a) respectively. Overall, the release rate and released amount of DOX at pH 5.0 were higher than that at pH 7.4, suggesting a promoted drug release behavior at tumor site. Because of the release of DOX from micelles is mainly by means of free diffusion, this distinction could be attributed to the solubility of DOX at different pH values as well as the electrostatic interaction between heparosan and DOX. As we known, DOX is well soluble at low pH in an ionized state. Thus, low pH facilitates the encapsulated DOX to migrate from the inner to outer shell, results in the increasing of release rate. Furthermore, at pH 5.0, the carboxyl groups of heparosan were discharged, desorption of DOX from the shell region of micelles was also promoted, and induced the rapid release behavior at the first 10 h. Additionally, the DOX-loaded micelles also showed an accelerated release behavior with the addition of β-glucuronidase. Over 65 percent of the DOX released out in the initial 10 h because of the degradation of heparosan. Since tumor bears many features including low pH and various over-expressed enzymes, the phenomena in drug release study demonstrated the HD micelle might perform a satisfied release behavior in tumor site.

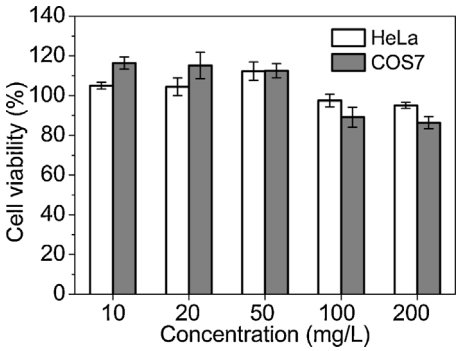

Fig. 5. *In vitro* cytotoxicity of HD against HeLa cells and COS7 cells. Error bars represent standard deviation of 3 replicates for the test.

3.4. In vitro cytotoxicity study

The cytotoxicity study of HD and DOX-loaded micelles were performed against HeLa and COS7 cell-lines by MTT assay. As exhibited in Fig. 5, HD behaves no significant cytotoxicity in both tumor and normal cells, and over 80% of cells survive after co-incubating with HD even at high concentration of 200 mg/L, showing good biocompatibility. Subsequently, the cytotoxicity of DOX-loaded micelles was evaluated. As shown in Fig. 6a, the half-maximal inhibitory concentration (IC50) of DOX-loaded micelles and free DOX against HeLa cells exhibited indistinctive difference. On the contrary, the IC50 value of DOX-loaded micelles against COS7 cells was much higher than that of free DOX (Fig. 6b), indicating a low cytotoxicity. Since the dose of DOX was the same, this difference may relate to the release behavior of DOX at different milieu. As illustrated in drug release profiles, the milieu like low pH and the presence of β-glucuronidase could facilitate the release of DOX from micelles. Because of the tumor cells met such conditions, this might lead to the accelerated release behavior of DOX, showing distinctive cytotoxicity against HeLa cells as compared with COS7 cells.

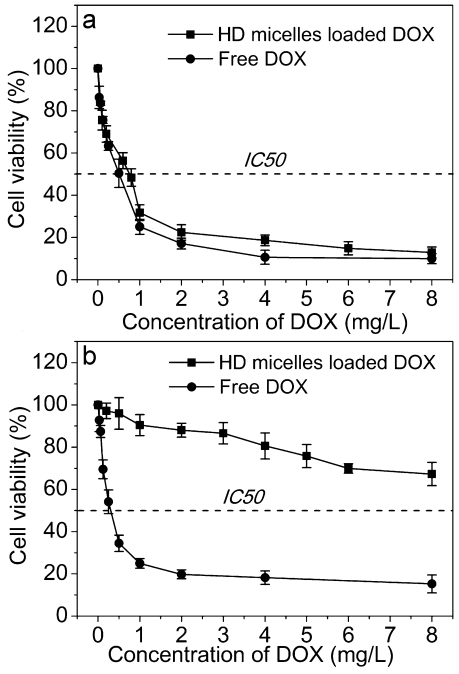

Fig. 6. *In vitro* cytotoxicity of DOX-loaded micelles and DOX against (a) HeLa cells and (b) COS7cells. Error bars represent standard deviation of 3 replicates for the test.

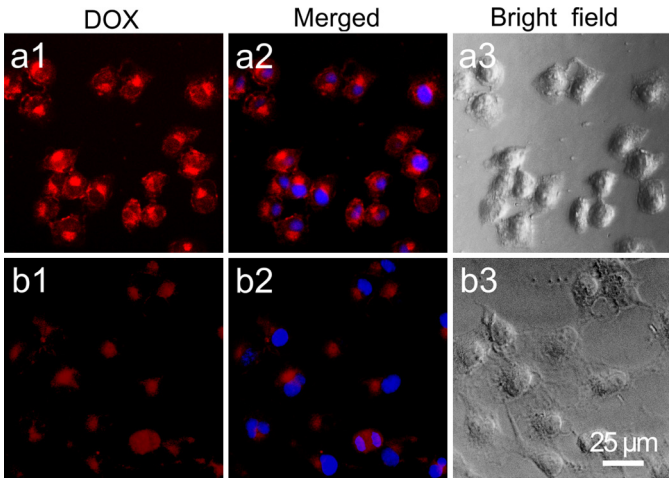

Fig. 7. Fluorescent images of (a) HeLa cells and (b) COS7 cells co-cultured with DOX-loaded micelles for 1 h. (a1, b1) Red fluorescence showed the DOX has internalized into cells; (a2, b2) blue represented cell nuclei stained by DAPI; (a3, b3) bright-field images. (For interpretation of the references to color in this figure legend, the reader is referred to the web version of the article.)

3.5. Cellular internalization

HeLa and COS7 cells were incubated with DOX-loaded micelles respectively to assess the cellular uptake of micelles. The distribution of red fluorescent DOX was observed by using an inverted fluorescence microscope. As presented in Fig. 7, the red spots corresponding to DOX were found in the cytoplasm of HeLa cells, illustrating that DOX-loaded micelles were successfully internalized (Fig. 7a1). In contrast, the red fluorescence in COS7 cells was weak (Fig. 7b1), showing that less DOX was delivered into COS7 cells. Given the hydrophobic property of DOX, it is reasonable to postulate that the effective uptake of DOX was achieved by the transporting of HD micelles. Besides, DAPI of blue fluorescence was utilized to label the cellular nuclei for further exploring the localization of DOX. From the merged fluorescence images (Fig. 7a2 and b2), the colocalization of red and blue fluorescence indicates that a number of DOX molecules have accumulated in the nuclei of HeLa cells. Furthermore, it was found from Fig. 7a3 and b3, HeLa cells emerged shrinking shape, while COS7 cells were of spreading morphology. These phenomena indicated that the state of HeLa cells is abnormal, which agree with the result of cytotoxicity assay. Since higher amount of DOX-loaded micelles were internalized by HeLa cells than that of COS7 cells, as shown in Fig. 7a1 and b1. This might also increase the different cytotoxic effect between tumor and normal cells.

4. Conclusions

A novel polymeric amphiphile based on heparosan and DOCA conjugate was prepared. DOCA as hydrophobic moieties could propel HD to form self-assembly micelles in aqueous medium and hydrophobic model drug DOX was effectively encapsulated in micelles. Since heparosan gathered on the shell region, the micelle had negatively charged surface and showed favorable stability in serum solution. The drug release study revealed the resulting micelles could achieve sustained drug release at pH 7.4, and accelerated drug release at pH 5.0 or in the existence of β-glucuronidase as well. Cellular uptake and *in vitro* cytotoxicity assay confirmed that DOX-loaded micelles could efficiently internalize into HeLa cells, and show significant distinction of IC50 between tumor cells and normal cells. Combined with good biocompatibility of HD and

abundant source of heparosan, the HD micelles developed here will have a great potential as drug carriers for cancer therapy.

Acknowledgments

This work was financially supported by the Doctoral Scientific Fund Project of the National Natural Science Foundation of China (51303068), Natural Science Fund of Jiangsu Province (BK2012557), Doctoral Scientific Fund Project of the Ministry of Education of China (20110093110008), and the Opening Fund of Key Laboratory of Biomedical Polymers, Ministry of Education, Wuhan University (20110401).

Appendix A. Supplementary data

Supplementary data associated with this article can be found, in the online version, at http://dx.doi.org/10.1016/j.carbpol.2014.03.084.

References

Baldwin, A. D., & Kiick, K. L. (2010). Polysaccharide-modified synthetic polymeric biomaterials. *Biopolymers*, *94*(1), 128–140.

Barzu, T., van Rijn, J. L., Petitou, M., Tobelem, G., & Caen, J. P. (1987). Heparin degradation in the endothelial cells. *Thrombosis Research*, *47*(5), 601–609.

Blanazs, A., Armes, S. P., & Ryan, A. J. (2009). Self-assembled block copolymer aggregates: From micelles to vesicles and their biological applications. *Macromolecular Rapid Communications*, *30*(4–5), 267–277.

Blundell, C. D., Roberts, I. S., Sheehan, J. K., & Almond, A. (2009). Investigating the molecular basis for the virulence of *Escherichia coli* K5 by nuclear magnetic resonance analysis of the capsule polysaccharide. *Journal of Molecular Microbiology and Biotechnology*, *17*(2), 71–82.

Brigger, I., Dubernet, C., & Couvreur, P. (2002). Nanoparticles in cancer therapy and diagnosis. *Advanced Drug Delivery Reviews*, *54*(5), 631–651.

Caliceti, P., & Veronese, F. M. (2003). Pharmacokinetic and biodistribution properties of poly(ethylene glycol)–protein conjugates. *Advanced Drug Delivery Reviews*, *55*(10), 1261–1277.

Chen, J. H., Avci, F. Y., Munoz, E. M., McDowell, L. M., Chen, M., Pedersen, L. C., et al. (2005). Enzymatic redesigning of biologically active heparan sulfate. *Journal of Biological Chemistry*, *280*(52), 42817–42825.

Clarke, B. R., Esumeh, F., & Roberts, I. S. (2000). Cloning, expression, and purification of the K5 capsular polysaccharide lyase (KflA) from coliphage K5A: Evidence for two distinct K5 lyase enzymes. *Journal of Bacteriology*, *182*(13), 3761–3766.

DeAngelis, P. L. (2013). HEPtune: A process of conjugating a naturally occurring sugar molecule, heparosan, to a drug for enhanced drug delivery. *Drug Development & Delivery*, *13*(1), 34–38.

Duncan, R. (2003). The dawning era of polymer therapeutics. *Nature Reviews Drug Discovery*, *2*(5), 347–360.

Ferrari, M. (2005). Cancer nanotechnology: Opportunities and challenges. *Nature Reviews Cancer*, *5*(3), 161–171.

Grinda, M., Clarhaut, J., Renoux, B., Tranoy-Opalinski, I., & Papot, S. (2012). A self-immolative dendritic glucuronide prodrug of doxorubicin. *MedChemComm*, *3*(1), 68–70.

Janes, K. A., Calvo, P., & Alonso, M. J. (2001). Polysaccharide colloidal particles as delivery systems for macromolecules. *Advanced Drug Delivery Reviews*, *47*(1), 83–97.

Karmali, P. P., & Simberg, D. (2011). Interactions of nanoparticles with plasma proteins: implication on clearance and toxicity of drug delivery systems. *Expert Opinion on Drug Delivery*, *8*(3), 343–357.

Kataoka, K., Harada, A., & Nagasaki, Y. (2001). Block copolymer micelles for drug delivery: Design, characterization and biological significance. *Advanced Drug Delivery Reviews*, *47*(1), 113–131.

Koo, H., Huh, M. S., Sun, I. C., Yuk, S. H., Choi, K., Kim, K., et al. (2011). In vivo targeted delivery of nanoparticles for theranosis. *Accounts of Chemical Research*, *44*(10), 1018–1028.

Langer, R., & Tirrell, D. A. (2004). Designing materials for biology and medicine. *Nature*, *428*(6982), 487–492.

Li, P. L., Sheng, J. Z., Liu, Y. H., Li, J., Liu, J., & Wang, F. S. (2013). Heparosan-derived heparan sulfate/heparin-like compounds: one kind of potential therapeutic agents. *Medicinal Research Reviews*, *33*(3), 665–692.

Liu, Z. H., Jiao, Y. P., Wang, Y. F., Zhou, C. R., & Zhang, Z. Y. (2008). Polysaccharides-based nanoparticles as drug delivery systems. *Advanced Drug Delivery Reviews*, *60*(15), 1650–1662.

Mizrahy, S., & Peer, D. (2012). Polysaccharides as building blocks for nanotherapeutics. *Chemical Society Reviews*, *41*(7), 2623–2640.

Moghimi, S. M., Hunter, A. C., & Murray, J. C. (2001). Long-circulating and target-specific nanoparticles: Theory to practice. *Pharmacological Reviews*, *53*(2), 283–318.

Otsuka, H., Nagasaki, Y., & Kataoka, K. (2003). PEGylated nanoparticles for biological and pharmaceutical applications. *Advanced Drug Delivery Reviews*, *55*(3), 403–419.

Park, K., Kim, K., Kwon, I. C., Kim, S. K., Lee, S., Lee, D. Y., et al. (2004). Preparation and characterization of self-assembled nanoparticles of heparin-deoxycholic acid conjugates. *Langmuir*, *20*(26), 11726–11731.

Peer, D., Karp, J. M., Hong, S., Farokhzad, O. C., Margalit, R., & Langer, R. (2007). Nanocarriers as an emerging platform for cancer therapy. *Nature Nanotechnology*, *2*(12), 751–760.

Raman, K., Mencio, C., Desai, U. R., & Kuberan, B. (2013). Sulfation patterns determine cellular internalization of heparin-like polysaccharides. *Molecular Pharmaceutics*, *10*(4), 1442–1449.

Riess, G. (2003). Micellization of block copolymers. *Progress in Polymer Science*, *28*(7), 1107–1170.

Rosler, A., Vandermeulen, G. W., & Klok, H. A. (2001). Advanced drug delivery devices via self-assembly of amphiphilic block copolymers. *Advanced Drug Delivery Reviews*, *53*(1), 95–108.

Simpson, C. A., Agrawal, A. C., Balinski, A., Harkness, K. M., & Cliffel, D. E. (2011). Short-chain PEG mixed monolayer protected gold clusters increase clearance and red blood cell counts. *ACS Nano*, *5*(5), 3577–3584.

Stark, W. J. (2011). Nanoparticles in biological systems. *Angewandte Chemie-International Edition*, *50*(6), 1242–1258.

Torchilin, V. P. (2001). Structure and design of polymeric surfactant-based drug delivery systems. *Journal of Controlled Release*, *73*(2–3), 137–172.

Volpi, N. (2004). Purification of the *Escherichia coli* K5 capsular polysaccharide and use of high-performance capillary electrophoresis to qualitative and quantitative monitor the process. *Electrophoresis*, *25*(18–19), 3307–3312.

Wang, B., He, X., Zhang, Z. Y., Zhao, Y. L., & Feng, W. Y. (2013). Metabolism of nanomaterials in vivo: Blood circulation and organ clearance. *Accounts Chemical Research*, *46*(3), 761–769.

Wang, Z. Y., Zhang, Z. Q., McCallum, S. A., & Linhardt, R. J. (2010). Nuclear magnetic resonance quantification for monitoring heparosan K5 capsular polysaccharide production. *Analytical Biochemistry*, *398*(2), 275–277.

Xu, X. D., Chen, J. X., Cheng, H., Zhang, X. Z., & Zhuo, R. X. (2012). Controlled peptide coated nanostructures via the self-assembly of functional peptide building blocks. *Polymer Chemistry*, *3*(9), 2479–2486.

Zhang, C. Y., Liu, L., Teng, L. P., Chen, J. H., Liu, J., Li, J. H., et al. (2012). Metabolic engineering of *Escherichia coli* BL21 for biosynthesis of heparosan, a bioengineered heparin precursor. *Metabolic Engineering*, *14*(5), 521–527.